Geomechanics and Engineering, *Vol. 18, No. 2 (2019) 141-151*
DOI: https://doi.org/10.12989/gae.2019.18.2.141

Structural response of historical masonry arch bridges under different arch curvature considering soil-structure interaction

Ahmet Can Altunışık*[1], Burcu Kanbur[1a], Ali Fuat Genç[2b] and Ebru Kalkan[1c]

[1]*Department of Civil Engineering, Karadeniz Technical University, Trabzon, Turkey*
[2]*Department of Civil Engineering, Karadeniz Technical University, Of Technology Faculty, Trabzon, Turkey*

(Received April 12, 2018, Revised May 10, 2019, Accepted May 13, 2019)

Abstract. In this paper, it is aimed to present a detail investigation about the comparison of static and dynamic behavior of historical masonry arch bridges considering different arch curvature. Göderni historical masonry two-span arch bridge which is located in Kulp town, Diyarbakır, Turkey is selected as a numerical application. The bridge takes part in bowless bridge group and built in large measures than the others. The restoration projects were approved and rehabilitation studies have still continued. Finite element model of the bridge is constituted with special software to determine the static and dynamic behavior. To demonstrate the arch curvature effect, the finite element model are reconstructed considering different arch curvature between 2.86 m-3.76 m for first arch and 2.64 m-3.54 m for second arch with the increment of 0.10 m, respectively. Dead and live vehicle loads are taken into account during static analyses. 1999 Kocaeli earthquake ground motion record is considered for time history analyses. The maximum displacements, principal stresses and elastic strains are compared with each other using contour diagrams. It is seen that the arch curvature has more influence on the structural response of historical masonry arch bridges. At the end of the study, it is seen that with the increasing of the arch heights, the maximum displacements, minimum principal stresses and minimum elastic strains have a decreasing trend in all analyses, in addition maximum principal stresses and maximum elastic strains have unchanging trend up to optimum geometry.

Keywords: arch bridge; dynamic behavior; finite element model; masonry; curvature effect

1. Introduction

Historical masonry arch bridges are the most common and oldest structural bridge form in architecture. Their history dates back to thousands of years (Altunışık *et al.* 2015a). With the innovation of the arch form, the history of masonry arch bridge was started. Being fairly convenient to span large distances, arches are designed to resist compressive forces and generally exposed to those forces due to their geometric shape. Because of this reason arches are commonly utilized in the masonry buildings Stone and brick material are used generally for the construction of arches since they have excessive compressive strength (Ural *et al.* 2008). In the process of time, the bridges were diversified and built with different size and shape such as one span, multi span, straight, curved etc. by many countries to expose the their own architecture style.

In time, masonry arch bridges have been damaged and collapsed because of some factors such as earthquakes, loss in the strength of construction materials, time-dependent deformations, excessive and irregular loading due to inconvenient use, support settlements, floods, fires, wars and vandalism (Toker and Unay 2004). Especially earthquakes, which is appear a sudden shaking of the earth caused by the breaking and shifting of rocks beneath the earth surface (Bayraktar *et al.* 2014), are more destructive than others. These factors affected the life of masonry bridges drastically. These bridges, which are bracelets of the rivers, have reached today through made restoration and repair applications.

Bridges are one of the most important engineering structures which are commonly used for transportation (Altunışık *et al.* 2012). Historical masonry arch bridges have supplied the requirements of human populations for years. They have also aesthetic appearance. But, with the innovations in structural engineering, the construction materials changed and use of stone, mortar, timber block etc. give place to steel and concrete. However, many historical masonry arch bridges have been used due to the inherent stability of arch form (Altunışık *et al.* 2015b). Also, some of them are located on route of railway and highway transportations and they support the traffic under potentially destructive conditions such as an increase in traffic loads and intense vibrations produced by the traffic. Therefore, these historical structures that designed for lower loads require special attention due to their changing functions to avoid deterioration and possible structural decay (Solla *et al.* 2012). In addition, natural disasters such as earthquakes damage masonry bridges which designed to

*Corresponding author, Professor
E-mail: ahmetcan8284@hotmail.com
[a]Ph.D. Student
E-mail: burcukanbur@hotmail.com
[b]Ph.D. Student
E-mail: af.genc@ktu.edu.tr
[c]Ph.D. Student
E-mail: ebrukalkan@ktu.edu.tr

Copyright © 2019 Techno-Press, Ltd.
http://www.techno-press.org/?journal=gae&subpage=7
ISSN: 2005-307X (Print), 2092-6219 (Online)

resist gravity loads, heavily and more attention is required against to earthquake movements.

Proper retrofitting of historical structures involves a comprehensive understanding of their structural pathology and behavior, before taking any intervention measures (Syrmakezis *et al.* 2008). In the literature many studies exist about the structural behavior of historical masonry arch bridges. At first, investigation of load bearing capacity of the masonry arch bridges had been assessed by researchers with considering geometry of the arches. For this purpose researches developed some empirical formulas. Trust line and middle third rule are first assessments about arches. In 1950s, during the World War II, the MEXE method developed for load carrying capacity of arch bridges depend on some assumptions and geometric properties (Bjurström and Lasell 2009). After the finite element method has developed, bridges are examined in every aspects as well as geometric effects. Drosopoulos *et al.* (2008) investigated the ultimate failure load of the stone arch with considered different arch heights. Oliveira *et al.* (2010) made limit analyses to examine the ultimate loads of masonry arch bridges considered different arch geometries. Arteaga and Morer (2012) made limit analyses to assess the effect of geometry on the structural capacity of masonry arch bridges with different geometric features. Sarhosis *et al.* (2014) examined the effect of the angle of skew on the load carrying capacity of single span stone masonry arches. Conde *et al.* (2016) investigated the influence of geometry on the collapse load estimation of the in-service mediaeval masonry arch bridge. It can be seen in the literature, almost every study that about geometric effects were made with limit analyses and the effects measured on load factors and ultimate loads.

The geometric properties, dimensions and forms of each structural element have very important effect on the structural behavior of engineering structures especially in historical masonry arch bridges. Already some structural analyses were made in literature for investigation of geometry effects on the structural behavior of masonry arch bridges but in these investigations arches and bridges were assessed with ultimate loads. It is seen from the literature that there is not any seismic investigations for assessing the geometry effect. For this purpose, this paper is presented to evaluate geometry effects with using static and seismic analyses. The changes in arch curvature, which is main structural element for masonry arch bridges, are considered for static and time-history seismic analyses. Ten different arch curvatures are evaluated under dead, live and earthquake loads by the increment of arch heights as 0.10 m. The maximum displacements, principal stresses and elastic strains are attained and compared with each other.

2. Göderni historical masonry arch bridge

Göderni historical masonry arch bridge is located on Kulp town in Diyarbakır, Turkey (Fig. 1). The bridge is dated back to 19th century and takes part in bowless bridge group. The bridge has two arches with 62.0 total length and 6.05 m width, respectively. The first and second arches have 12.00 m and 11.85 m maximum spans, 3.04 m and 3.26 m heights, 7.54 m and 9.35 m radius, and 0.52 m and 0.69 m arch thickness, respectively.

Fig. 1 Göderni two-span historical masonry arch bridge

There are some hazardous conditions for the bridge such as damages of arches, walls and pavements, ruptures of stone pieces, environmental problems, deteriorations in expansion joints, scour at abutments, and filling of side slopes. Fig. 2 shows these deteriorative and hazardous conditions. The restoration projects were approved by General Directorate of Highways and rehabilitation studies have still continued. It is planned to using for pedestrian crossings and vehicle traffic after restoration.

The structural elements such as arches and side walls of the bridge were generally built by cut stone. The timber block was consisted with different sizes of limestone, sand, and gravel. The cement-based mortar was used as a binding material. Stone and mortar samples were taken from the bridge for testing in the laboratory to determine the mechanical properties of materials (Bayraktar 2013). As a result of laboratory tests, the compressive strength and weight per unit volume were attained as 30-50 MPa and 2000-2400 kg/m^3 for stones, respectively. Also, the compressive strength of mortar was calculated between 4.0 and 9.0 MPa.

3. Static and dynamic behavior considering different arch curvature

Finite element model of the bridge is constituted in ANSYS software (ANSYS 2014) using relievo drawings to determine the static and dynamic behavior. General information, structural dimensions, material properties and some additional information were obtained from the Abdulkadir Aslan Engineering Company and Technical report (2013). To demonstrate the arch curvature effect, the finite element model are reconstructed considering different arch curvature between 2.86 m-3.76 m for first arch and 2.64 m-3.54 m for second arch with the increment of 0.10

Fig. 2 Deteriorative and hazardous conditions of the bridge

Table 1 Arch heights of different analyses cases

Analyses Cases	Arch Heights (m)	
	First Arch	Second Arch
1	2.86	2.64
2	2.96	2.74
3	3.06	2.84
4	3.16	2.94
5	3.26	3.04
6	3.36	3.14
7	3.46	3.24
8	3.56	3.34
9	3.66	3.44
10	3.76	3.54

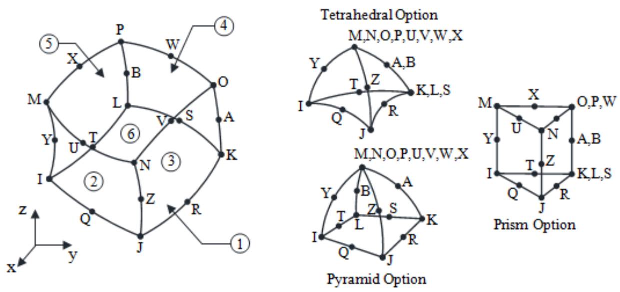

Fig. 3 Structural solid geometry of SOLID186 element

m, respectively. Table 1 summarized the analyses cases and related arches heights.

The finite element modeling of historical masonry structures can be classified into three groups as micro modeling, simplified micro modeling and macro modeling. In the micro modeling method, the material properties of the masonry unit and mortar forming the masonry wall are evaluated separately. In the simplified micro modeling method, the masonry units are extended by half the thickness of the mortar layer and the mortar layer is neglected and the masonry units are separated from each other by the interface lines. In the macro modeling method, there is no distinction between stone/brick units and mortar. The structural components are considered as composite. An equivalent material model is used to reflect the common character of these materials. In this paper, macro modelling method is used in the static and dynamic analyses.

Dead and live loads (vehicle) are taken into account during static analyses. 1999 Kocaeli earthquake ground motion record is considered for time history analyses. The maximum displacements, principal stresses and elastic strains are compared with each other using contour diagrams. The results are presented for Case 1 with contour diagrams and compared with Case 2-10 using tables and comparison graphics.

In the finite element models of the bridge, SOLID186 element type having 20 node and three degrees of freedom per node as translations in the nodal x, y, and z directions. In addition, it has the capability of plasticity, elasticity, creep, stress stiffening, large deflection, and large strains. This element has tetrahedral, pyramid and prism options for meshing. Fig. 3 shows the structural solid geometry of this element type. SOLID186 cannot be used for nonlinear analyses. SOLID65 element type is more suitable and can be used for nonlinear analyses.

Three dimensional finite element model of the bridge considered dimensions for Case 1 is given in Fig. 4. All boundary conditions are considered to be fixed in the model. Finite element models are constituted as macro modeling technic which preferred for large scale masonry structures. In this technic, stone, mortar and interfaces are modeled as a homogeneous continuum medium. The material properties are taken considering the homogenized masonry units (Lourenço 1996). In this paper static and dynamic analyses are performed to be linear elastic.

Determining the material properties of masonry units that assumed in the analyses as homogeneous continuum medium is very difficult. To obtain those properties, full scale laboratory tests or in field experimental tests should

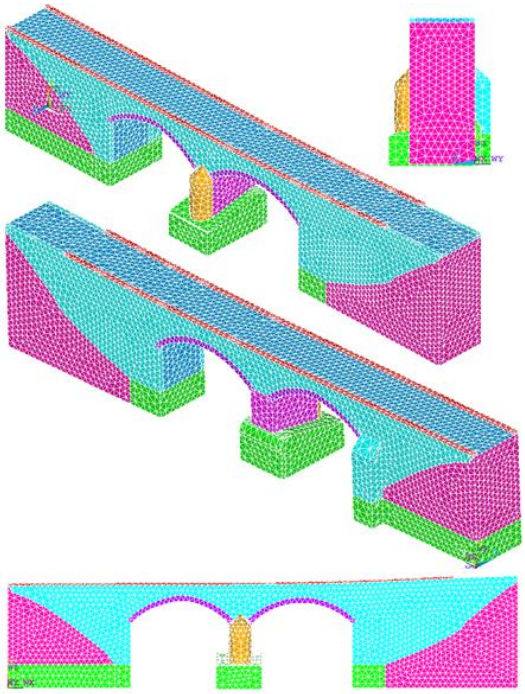

Fig. 4 Three dimensional finite element model of the bridge for Case 1

Table 2 Material properties used in the analysis

Structural Elements	Material Properties		
	Modulus of Elasticity (N/m^2)	Poisson Ratio (-)	Density (kg/m^3)
First Arch	5.00E9	0.20	2000
Second Arch	5.00E9	0.20	2000
Side Walls	3.00E9	0.20	2000
Timber Blocks	6.0E08	0.20	1800
Abutments	5.00E9	0.20	2000
Cutwaters	5.00E9	0.20	2000
Slopes	7.00E9	0.20	2500
Foundations	7.00E9	0.20	2500

be made. However these tests are both difficult and non-allowable due to historic value of the bridge. Therefore no experimental study was made with regard to the material characteristic of the masonry walls and arches. The material characteristics are taken to be similar to those available in the literature. In the literature, different material properties are used for masonry structures (Carpinteri *et al.* 2005, Betti *et al.* 2011, Saloustros *et al.* 2015, Altunışık *et al.* 2016, Angin 2016). The material properties of masonry elements given in Table 2 are selected from between these ranges.

3.1 Static analyses under Dead Load (G)

The maximum vertical displacements contour diagram of the bridge attained from static analyses under dead load is shown in Fig. 5(a). It is seen that the displacements have an increasing trend from the side edges and middle pier to middle point of arches. The maximum values of displacements are attained as 2.26 mm and 1.67 mm for first and second arches, respectively.

The maximum principal stress contour diagram of the bridge attained from static analyses under dead load is shown in Fig. 5(b). It is seen that local stress locations are obtained at transition points between side supports and bridge as 0.72 MPa. Also, some stress accumulations regions are observed at side walls, inner sides of arches and some parts of parapets as 0.55 MPa. Beside these regions, the maximum principal stresses reached the values of 0.15 MPa.

The minimum principal stress contour diagram of the bridge attained from static analyses under dead load is shown in Fig. 5(c). It is seen that local stress locations are obtained at damaged side walls and contact surface between the lower parts of arches and pier/side abutments as 2.82 MPa. Also, some stress accumulations regions are observed at intersection lines between arches and side walls, bottom surface of side slopes and middle pier foundation as 1.50 MPa. Beside these regions, the minimum principal stresses reached the values of 0.61 MPa.

The maximum and minimum elastic strains contour diagrams of the bridge attained from static analyses under dead load are shown in Fig. 5(d). It is seen that local elastic strains are attained as 0.23E-3 and -0.81E-3, respectively. Also, some strain accumulations regions are observed with 0.11E-3 maximum value at the damaged side walls, inner sides of arches, upper side of pier and 0.18E-3 minimum value at the contact surfaces between arches and side walls on pier and pavement.

3.2 Static analyses under Dead and Live Load (GQ)

Considering the dead and live loads such as human and vehicle, the pressure load is taken into account as 1500 kg/m^2 and applied to the bridge deck during analyses. The maximum vertical displacements contour diagram of the bridge attained from static analyses under dead and live loads is shown in Fig. 6(a). It can be seen from the Fig. 6(a) that the displacements have an increasing trend from the side edges and middle pier to middle of the arch span. The maximum values of displacements are attained as 2.72 mm and 2.12 mm for first and second arches, respectively.

The maximum principal stress contour diagram of the bridge attained from static analyses under dead and live loads is shown in Fig. 6(b). It is seen that local stress locations are obtained at transition points between side supports and bridge as 0.83MPa. Also, some stress accumulations regions are observed at side walls, inner sides of arches and some parts of parapets as 0.55 MPa. Beside these regions, the maximum principal stresses reached the values of 0.17 MPa.

The minimum principal stress contour diagram of the bridge attained from static analyses under dead and live loads is shown in Fig. 6(c). It is seen that local stress locations are obtained at damaged side walls and contact surface between the lower parts of arches and pier/side abutments as 3.43 MPa. Also, some stress accumulations regions are observed at intersection lines between arches and side walls, bottom surface of side slopes and middle pier foundation as 1.35 MPa. Beside these regions, the minimum principal stresses reached the values of 0.60 MPa.

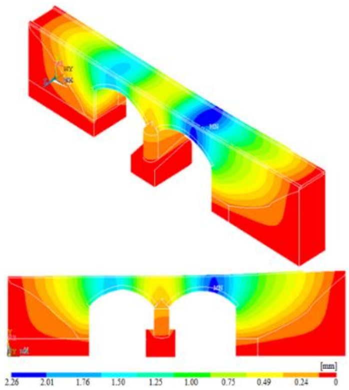

(a) Maximum displacement

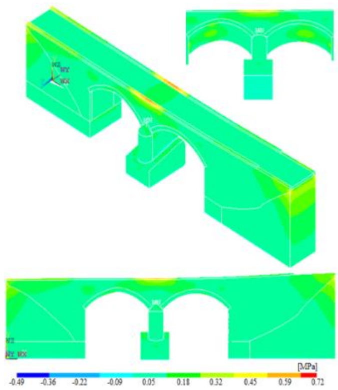

(b) Maximum principal stresses

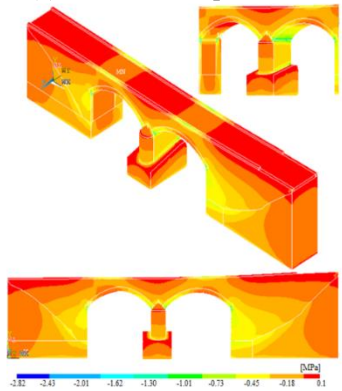

(c) Minimum principal stresses

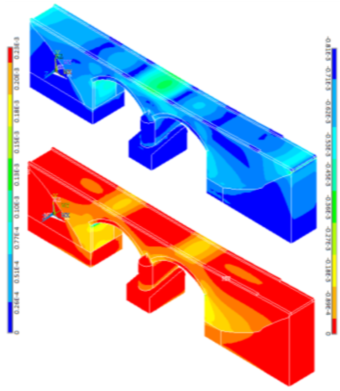

(d) Elastic strain

Fig. 5 Contour diagrams for static analyses under dead load

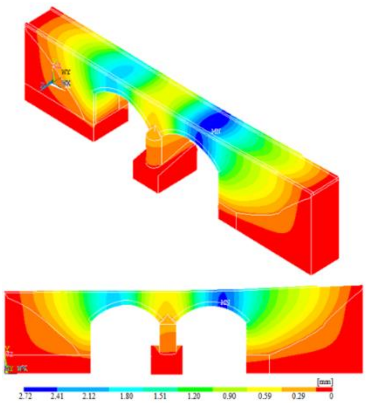

(a) Maximum displacement

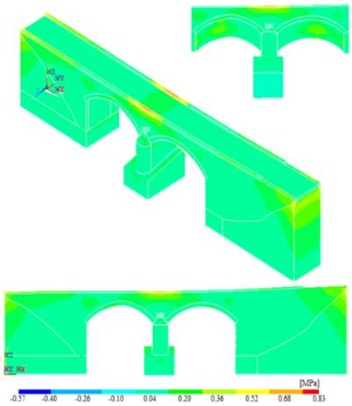

(b) Maximum principal stresses

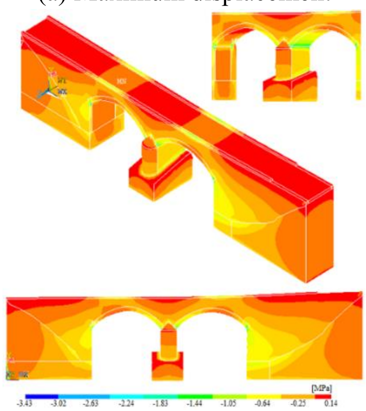

(c) Minimum principal stresses

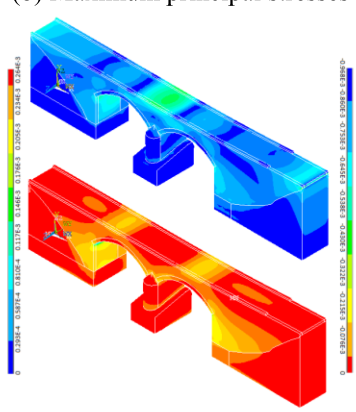

(d) Elastic strain

Fig. 6 Contour diagrams for static analyses under dead and live loads

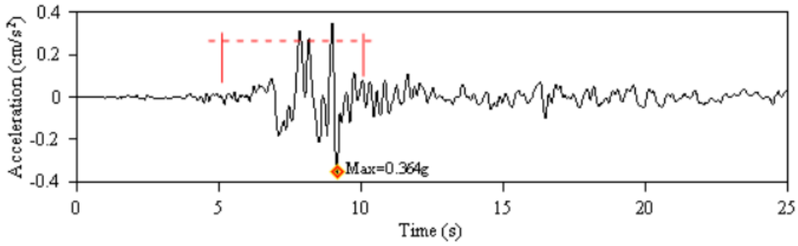

Fig. 7 1999 Kocaeli earthquake ground motion record obtained from Düzce station

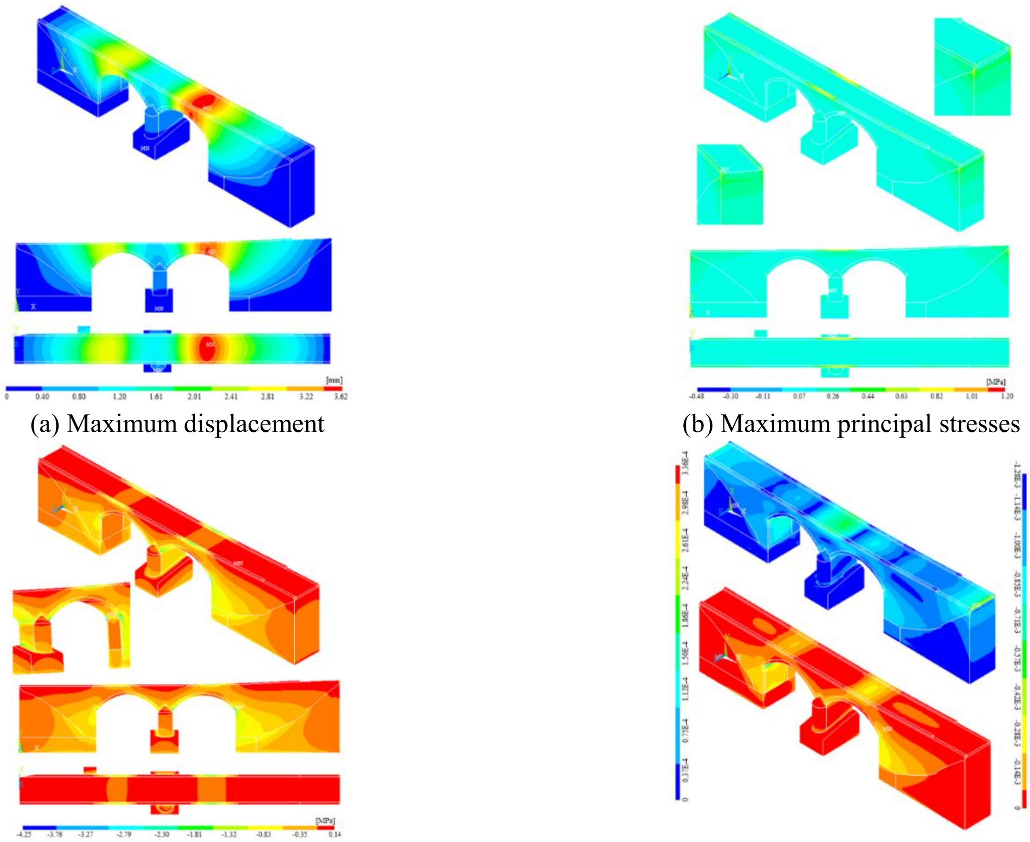

(a) Maximum displacement (b) Maximum principal stresses

(c) Minimum principal stresses (d) Elastic strain

Fig. 8 Contour diagrams for dynamic analyses under dead, live and earthquake loads

The maximum and minimum elastic strains contour diagrams of the bridge attained from static analyses under dead and live loads are shown in Fig. 6(d). It is seen that local elastic strains are attained as 0.26E-3 and -0.97E-3, respectively. Also, some strain accumulations regions are observed with 0.14E-3 maximum value at the damaged side walls, inner sides of arches, upper side of pier and -0.22E-3 minimum value at the contact surfaces between arches and side walls on pier and pavement.

3.3 Dynamic earthquake analyses under Dead, Live and Earthquake Loads (GQE))

To determine the dynamic earthquake behavior of the bridge, 1999 Kocaeli earthquake ground motion record (Fig. 7) obtained from Düzce station (PEER 2016) was selected and applied to the first mode direction considering dead and live loads. Because of the computational demand and less time consuming, only five seconds between 5 sn and 10sn of the record, which is the most effective duration, was taken into account.

The maximum displacements contour diagram of the bridge attained from dynamic analyses under dead, live and earthquake loads is shown in Fig. 8(a). It is seen that the displacements have an increasing trend from side edges and middle pier to middle point of the arch span. The displacements reach the maximum values at the middle of the first and second arches as 3.62 mm and 2.81 mm, respectively.

The maximum principal stress contour diagram of the bridge attained from dynamic analyses under dead, live and earthquake loads is shown in Fig. 8(b). It is seen that local stress locations are obtained at transition points between side supports and bridge as 1.20 MPa. At the upper side of the pier, on parapets, maximum 0.82 MPa stress occurred. Beside these regions, the maximum principal stresses reached the values of 0.26 MPa.

The minimum principal stress contour diagram of the

Table 3 Analyses results for different arch curvature under dead load

Arch Heights (m)	Displacements (mm)	Analysis Results –Dead Load (G)			
		Stresses (MPa)		Strains (--)	
		Maximum	Minimum	Maximum	Minimum
2.86-2.64	2.26	0.73	2.82	2.31E-4	8.10E-4
		0.05	0.22	0.26E-4	0.90E-4
2.96-2.74	2.23	0.73	2.65	2.31E-4	7.96E-4
		0.05	0.21	0.26E-4	0.88E-4
3.06-2.84	2.19	0.73	2.51	2.31E-4	7.80E-4
		0.06	0.19	0.26E-4	0.87E-4
3.16-2.94	2.16	0.73	2.26	2.31E-4	7.54E-4
		0.08	0.16	0.26E-4	0.84E-4
3.26-3.04	2.13	0.72	2.11	2.32E-4	7.40E-4
		0.08	0.15	0.26E-4	0.82E-4
3.36-3.14	2.09	0.73	1.99	2.32E-4	6.89E-4
		0.09	0.13	0.26E-4	0.76E-4
3.46-3.24	2.06	0.73	1.92	2.32E-4	6.74E-4
		0.09	0.05	0.26E-4	0.75E-4
3.56-3.34	2.03	0.94	1.89	2.87E-4	6.58E-4
		0.09	0.12	0.32E-4	0.73E-4
3.66-3.44	2.01	0.94	1.80	2.88E-4	6.54E-4
		0.09	0.03	0.32E-4	0.73E-4
3.76-3.54	1.99	0.95	1.79	2.88E-4	6.53E-4
		0.12	0.03	0.32E-4	0.73E-4

Table 4 Analyses results for different arch heights under dead and live loads

Arch Heights (m)	Displacements (mm)	Analysis Results –Dead and Live Load (GQ)			
		Stresses (MPa)		Strains (--)	
		Maximum	Minimum	Maximum	Minimum
2.86-2.64	2.72	0.83	3.43	2.64E-4	9.68E-4
		0.01	0.28	0.17E-4	1.00E-4
2.96-2.74	2.66	0.83	3.22	2.65E-4	9.84E-4
		0.05	0.17	0.17E-4	1.00E-4
3.06-2.84	2.63	0.83	3.07	2.65E-4	9.88E-4
		0.06	0.24	0.17E-4	1.10E-4
3.16-2.94	2.60	0.83	2.78	2.65E-4	9.29E-4
		0.06	0.21	0.17E-4	1.10E-4
3.26-3.04	2.57	0.83	2.60	2.65E-4	9.16E-4
		0.06	0.19	0.17E-4	1.10E-4
3.36-3.14	2.53	0.83	2.42	2.65E-4	8.56E-4
		0.07	0.17	0.18E-4	0.95E-4
3.46-3.24	2.50	1.04	2.35	3.16E-4	8.41E-4
		0.07	0.15	0.23E-4	0.93E-4
3.56-3.34	2.47	1.05	2.31	3.16E-4	8.22E-4
		0.08	0.07	0.23E-4	0.91E-4
3.66-3.44	2.44	1.05	2.20	3.17E-4	8.17E-4
		0.09	0.05	0.23E-4	0.91E-4

Table 4 Continued

Arch Heights (m)	Displacements (mm)	Stresses (MPa) Maximum	Stresses (MPa) Minimum	Strains (--) Maximum	Strains (--) Minimum
3.76-3.54	2.38	1.05	2.17	3.17E-4	8.10E-4
		0.12	0.05	0.23E-4	0.90E-4

Analysis Results –Dead and Live Load (GQ)

Table 5 Analyses results for different arch heights under dead, live and earthquake loads

Arch Heights (m)	Displacements (mm)	Stresses (MPa) Maximum	Stresses (MPa) Minimum	Strains (--) Maximum	Strains (--) Minimum
2.86-2.64	3.62	1.20	4.25	3.36E-4	1.28E-3
		0.09	0.62	0.49E-4	0.22E-3
2.96-2.74	3.55	1.19	4.01	3.34E-4	1.26E-3
		0.13	0.49	0.48E-4	0.19E-3
3.06-2.84	3.51	1.18	3.86	3.33E-4	1.21E-3
		0.13	0.57	0.47E-4	0.18E-3
3.16-2.94	3.46	1.17	3.56	3.34E-4	1.20E-3
		0.13	0.54	0.48E-4	0.20E-3
3.26-3.04	3.42	1.16	3.38	3.37E-4	1.19E-3
		0.13	0.52	0.49E-4	0.20E-3
3.36-3.14	3.36	1.15	3.20	3.29E-4	1.13E-3
		0.13	0.50	0.46E-4	0.18E-3
3.46-3.24	3.31	1.34	3.13	3.78E-4	1.06E-3
		0.13	0.49	0.50E-4	0.16E-3
3.56-3.34	3.25	1.33	3.09	3.84E-4	1.10E-3
		0.14	0.41	0.53E-4	0.18E-3
3.66-3.44	3.19	1.32	2.98	3.81E-4	1.09E-3
		0.15	0.40	0.52E-4	0.18E-3
3.76-3.54	3.10	1.30	2.95	3.75E-4	1.08E-3
		0.18	0.40	0.49E-4	0.10E-3

Analysis Results –Dead, Live and Earthquake Loads (GQE)

bridge attained from dynamic analyses under dead, live and earthquake loads is shown in Fig. 8(c). It is seen that local stress locations are obtained at damaged side walls and contact surface between the lower parts of arches and pier/side abutments as 4.25MPa. Also, there are some stress accumulations regions with 1.81MPa stress value at the middle part of the spans. Beside these regions, the minimum principal stresses reached the values of 0.83MPa.

The maximum and minimum elastic strains contour diagrams of the bridge attained from dynamic analyses under dead, live and earthquake loads are shown in Fig. 8(d). It is seen that local elastic strains are attained as 3.36E-4 and -1.28E-3, respectively. Also, some strain accumulations regions are observed with 1.86E-4 maximum value at the damaged side walls, inner sides of arches, upper side of pier and -0.28E-3 minimum value at the contact surfaces between arches and side walls on pier and pavement.

Tables 3-5 summarized the maximum displacements, principal stresses and strains for all analyses cases (see Table 1) considering deal load (G), dead and live loads (GQ) and earthquake loads including dead and live loads (GQE), respectively.

It is seen that there are two values for stresses and strains. The bold characters are used to indicate the local peak values which cannot show the current and real responses. The normal characters indicate the reasonable and general responses of the bridge. It is concluded that these values can be used for comparison with limit boundaries.

The changing of maximum displacements, maximum-minimum principal stresses and maximum-minimum elastic strains with different arch heights under dead, live and earthquake loads are given with charts in Figs. 9(a)-9(e).

There is good correlation between arch heights and displacements, namely maximum displacements decrease when the arch heights increase. Maximum displacements decreased nearly about 12%, 12.5% and 14.4% for dead,

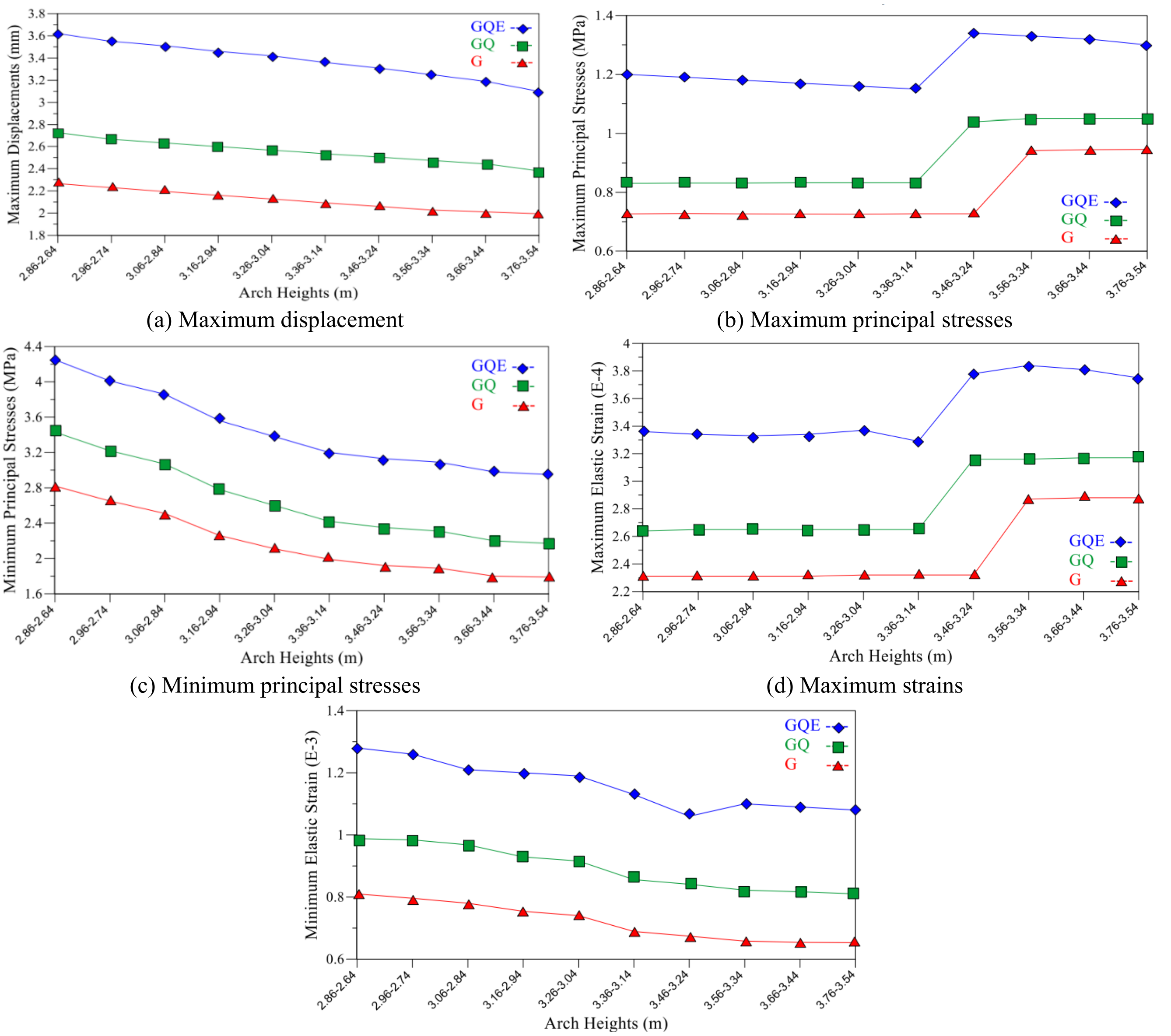

(a) Maximum displacement

(b) Maximum principal stresses

(c) Minimum principal stresses

(d) Maximum strains

(e) Minimum strain

Fig. 9 Changing of maximum displacements, principal stresses and elastic strains with different arch curvature under dead, live and earthquake loads

dead-live and dead-live-earthquake loads depend to increasing of arch heights, respectively (Fig. 9(a)).

From the Fig. 9(b), it is seen that the maximum principal stresses are nearly equal for first seven arch heights for dead load and first six arch heights for dead-live loads. Then the values are increased from 0.727 MPa to 0.942 MPa for dead load, and from 0.833 MPa to 1.04MPa for dead-live loads. The rest values continue nearly as a same value for each analysis. In the earthquake analyses, maximum stresses decreased from 1.20 MPa to 1.15 MPa up to sixth analysis than sharply increased the value of 1.34 MPa in the next analysis. Stresses decreased regularly in the rest of the analyses up to 1.30 MPa.

From the Fig. 9(c), it is seen that the minimum principal stress values decreased gradually owing to increasing the arch heights. The values decreased from 2.82 MPa to 1.79 MPa for dead load analyses, from 3.43 MPa to 2.17 MPa for dead-live loads and from 4.25 MPa to 2.95 MPa for dead-live-earthquake loads analyses.

From the Fig. 9(d), it can be seen that maximum elastic strain values are nearly equal for first seven arch heights for dead load analyses and first six arch heights for dead-live loads and dead-live-earthquake loads analyses. After these straight curves, there are big increases from 0.232E-3 to 0.287E-3 for dead load, from 0.265E-3 to 0.316E-3 for dead-live loads and from 3.29E-4 to 3.78E-4 for dead-live-earthquake loads analyses. The rest values continue nearly as a same value for each analysis.

From the Fig. 9(e), it can be seen that minimum elastic strain values. It is seen that three analysis results have a decreasing trend. The values decreased from 0.810E-3 to 0.653E-3 for dead load analyses, from 0.988E-3 to 0.810E-3 for dead-live loads analyses and from 1.28E-3 to 1.08E-3 for dead-live-earthquake loads analyses.

4. Conclusions

The purpose of this study is to investigate the arch height effects on the structural behavior of masonry arch bridge. For this purpose Göderni masonry arch bridge is chosen. Firstly finite element model of the bridge is constructed. Then the arch heights are increased gradually nine times and finite element models are reconstructed. The results are obtained for all arch heights under dead load, dead-live loads and dead-live-earthquake loads. Maximum displacements, maximum-minimum principal stresses and maximum-minimum elastic strains are given with counter diagrams and tables. Thanks to charts the results are compared and the arch height effect is determined. As a result of the study the following observations are made:

• The maximum displacements decreased when the arch heights were increased and this is true for reverse conditions.

• The maximum principal stresses nearly did not change with the increasing of the arch heights up to a point. Then big increasing occurred in the stresses for three analyses. Maximum values of the stresses occurred at transition points between side supports and bridge.

• The minimum principal stresses decreased when the arch heights increased for each analysis. This is likely due to reduction of the backfill volume so reduction of the weights with the increasing of the arch heights. Maximum values of the minimum principal stresses occurred at the damaged side walls and contact surface between the lower parts of arches and pier/side abutments.

• Similar to maximum elastic stresses, the maximum elastic strain values didn't change when the arch heights were increased up to a point. Then big increasing occurred in the strains each analysis.

• The minimum elastic strains decreased dependent on increasing the arch heights.

According to the results, increasing of the heights (increase of the height to span ratio) cause a decrease in displacements and compressive stresses in addition unchanging of the tensile stresses up to a point. Then an unwanted situation for masonry arches aroused with increased the tensile stresses. When assessing the results, this point assumable as "optimum geometry" for this bridge.

From the study, it can be seen that the arch heights influences are very important for the structural behavior of the masonry bridge. Therefore all parameters should be investigated to obtain "optimum geometry" for the bridges in the new constructions, restorations and strengthening applications. Other parameters of the bridge such as span width, pier width and height, backfill, arch thickness and skew angle of arch should be study for to understand the comprehensive behavior of the arch bridges.

Structural identification of historical masonry arch bridge based on finite element analysis is very complex problem due to some uncertain parameters accepted in numerical analyses such as material properties, boundary condition, damages etc. So, ambient vibration based non-destructive experimental measurement should be conducted on selected bridge before restoration to determine the initial condition. After restoration, experimental measurements should be repeated to verify the project success.

References

Altunisik, A.C., Bayraktar, A. and Genc, A.F. (2015a), "Determination of the restoration effect on the structural behavior of masonry arch bridges", *Smart Struct. Syst.*, **16**(1), 101-139. https://doi.org/10.12989/sss.2012.10.2.131.

Altunisik, A.C., Bayraktar, A. and Genc, A.F. (2016), "A study on seismic behaviour of masonry mosques after restoration", *Earthq. Struct.*, **10**(6), 1331-1346. http://doi.org/10.12989/eas.2016.10.6.1331.

Altunisik, A.C., Bayraktar, A. and Ozdemir, H. (2012), "Seismic safety assessment of Eynel Highway steel bridge using ambient vibration measurements", *Smart Struct. Syst.*, **10**(2), 131-154.

Altunisik, A.C., Kanbur, B. and Genc, A.F. (2015b), "The effect of arch geometry on the structural behavior of masonry bridges", *Smart Struct. Syst.*, **16**(6), 1069-1089. http://doi.org/10.12989/sss.2015.16.6.1069.

Angin, Z. (2016), "Geotechnical field investigation on Giresun hazelnut licenced warehause and spot exchange", *Geomech. Eng.*, **10**(4), 547-563. https://doi.org/10.12989/gae.2016.10.4.547.

ANSYS. (2014), *Swanson Analysis System*, Pennsylvania, U.S.A.

Bayraktar, A. (2013), *Diyarbakır-Kulp/Göderni Köprüsü'nün Yapısal Güvenlik Değerlendirme Raporu*, General Directorate of Highways, Ankara, Türkiye.

Bayraktar, A., Altunişik, A.C. and Muvafik, M. (2014), "Damages of minarets during Erciş and Edremit Earthquakes, 2011 in Turkey", *Smart Struct. Syst.*, **14**(3), 479-499. https://doi.org/10.12989/sss.2014.14.3.479.

Betti, M. and Vignoli, A. (2011), "Numerical assessment of the static and seismic behaviour of the basilica of Santa Maria all'Impruneta (Italy)", *Construct. Build. Mater.*, **25**(12), 4308-4324. https://doi.org/10.1016/j.conbuildmat.2010.12.028.

Bjurström, H. and Lasell, J. (2009), "Capacity assessment of a single span arch bridge with backfill: A case study of the Glomman Bridge", Ms.C Dissertation, KTH, Royal Institute of Technology, Stockholm, Sweden.

Carpinteri, A., Invernizzi, S. and Lacidogna, G. (2005), "In situ damage assessment and nonlinear modelling of a historical masonry tower", *Eng. Struct.*, **27**(3), 387-395. https://doi.org/10.1016/j.engstruct.2004.11.001.

Conde, B., Díaz-Vilariño, L., Lagüela, S. and Arias, P. (2016), "Structural analysis of Monforte de Lemos masonry arch bridge considering the influence of the geometry of the arches and fill material on the collapse load estimation", *Construct. Build. Mater.*, **120**(1), 630-642. https://doi.org/10.1016/j.conbuildmat.2016.05.107.

De Arteaga, I. and Morer, P. (2012), "The effect of geometry on the structural capacity of masonry arch bridges", *Construct. Build. Mater.*, **34**, 97-106. https://doi.org/10.1016/j.conbuildmat.2012.02.037.

Drosopoulos, G.A., Stavroulakis, G.E. and Massalas, C.V. (2008), "Influence of the geometry and the abutments movement on the collapse of stone arch bridges", *Construct. Build. Mater.*, **22**(3), 200-210. https://doi.org/10.1016/j.conbuildmat.2006.09.001.

Lourenco, P.B. (1996), *Computational Strategies for Masonry Structures*, Delft University Press, Delft, The Netherlands.

Oliveira, D.V., Lourenço, P.B. and Lemos, C. (2010), "Geometric issues and ultimate load capacity of masonry arch bridges from the northwest Iberian Peninsula", *Eng. Struct.*, **32**(12), 3955-3965. https://doi.org/10.1016/j.engstruct.2010.09.006.

PEER, (2016), Pacific Earthquake Engineering Research Center, University of California, Berkeley, California, U.S.A.

Saloustros, S., Pelà, L., Roca, P. and Portal, J. (2015), "Numerical

analysis of structural damage in the church of the Poblet monastery", *Eng. Fail. Anal.*, **48**, 41-61. https://doi.org/10.1016/j.engfailanal.2014.10.015.
Sarhosis, V., Oliveira, D.V., Lemos, J.V. and Lourenço, P.B. (2014), "The effect of skew angle on the mechanical behaviour of masonry arches", *Mech. Res. Commun.*, **61**, 53-59. https://doi.org/10.1016/j.mechrescom.2014.07.008.
Solla, M., Lorenzo, H., Novo, A. and Caamaño, J.C. (2012), "Structural analysis of the Roman Bibei bridge (Spain) based on GPR data and numerical modelling", *Automat. Construct.*, **22**, 334-339.
Syrmakezis, C.A., Antonopoulos, A.K. and Mavrouli, O.A. (2008), "Aseismic protection of historical structures using modern retrofitting techniques", *Smart Struct. Syst.*, **4**(2), 233-245. https://doi.org/10.12989/sss.2008.4.2.233.
Technical Report. (2013), *Tarihi Göderni Köprüsü Teknik Raporu*, General Directorate of Highways, Diyarbakır, Turkey.
Toker, S. and Unay, A.I. (2004), "Mathematical modeling and finite element analysis of masonry arch bridges", *Gazi Univ. J. Sci.*, **17**(2), 129-139.
Ural, A., Oruç, Ş., Doğangün, A. and Tuluk, Ö.İ. (2008), "Turkish historical arch bridges and their deteriorations and failures", *Eng. Fail. Anal.*, **15**(1-2), 43-53. https://doi.org/10.1016/j.engfailanal.2007.01.006.

CC